Electrical tuning of birefringence in silicon waveguides

K. K. Tsia, S. Fathpour, and B. Jalali[a)]
Electrical Engineering Department, University of California, Los Angeles, California 90095-1594, USA

(Received 18 December 2007; accepted 28 January 2008; published online 14 February 2008)

We demonstrate dynamic control of the birefringence in a silicon waveguide. Electrically tunable stress on the waveguide core is induced using an integrated piezoelectric film. We show that the induced birefringence can be used to fine tune the phase mismatch among interacting waves present in parametric nonlinear optical effects. © *2008 American Institute of Physics*. [DOI: 10.1063/1.2883925]

Birefringence describes an optical medium's anisotropic propagation constant. In other words, the material exhibits different refractive indices with respect to one or more optical axes. This phenomenon is widely used in electro-optic modulators, color filters, wave plates, optical axis gratings, liquid crystal displays, etc.

In an optical waveguide, birefringence leads to a relative phase shift between orthogonally polarized light beams, a property that can be exploited for phase matching in nonlinear optical interactions.[1] Many useful optical devices such as wavelength converters, parametric amplifiers, and oscillators require phase matching for efficient operation. This means that the interacting waves must travel in phase through the nonlinear medium. However, chromatic dispersion causes relative phase mismatches among the waves and hence it degrades the strength of the desired interaction. Chromatic dispersion can be compensated using the modal birefringence in optical waveguides.[1,2] However, this approach requires precise control of the birefringence, a task that cannot be achieved with control of waveguide dimensions alone since this will place stringent requirements on fabrication tolerances.[1] The ability to electrically vary the birefringence of an optical waveguide would, therefore, be of immense value as it would make it possible to achieve phase matching even in the presence of fabrication-induced uncertainties in waveguide dimensions. It will also make it possible to dynamically control both the linear and nonlinear interactions within a waveguide. A particularly intriguing capability offered by such a technology is adaptive control of the optical response using electronic intelligence.

In this paper, we report preliminary results on electronic tuning of the birefringence in a silicon waveguide. This is achieved by applying electrically tunable stress using an integrated piezoelectric transducer that blankets the waveguide.

Previously, the stress induced by a silicon dioxide cladding layer has been used to eliminate the modal birefringence in silicon-on-insulator (SOI) waveguides.[3] Similarly, silicon nitride has been employed as a straining cladding layer to break the inversion symmetry of the silicon crystal and, thus, exhibits linear electrooptic effect.[4] The stress induced by such strained dielectric cladding layers is static. In other words, it is not dynamically tunable. Direct application of mechanical stress via a load cell has been reported for dynamic tuning of the modal birefringence.[5] While this approach was useful in demonstrating the concept, the use of an external load cell is not a practical approach from the packaging size and cost viewpoints. The integration of a piezoelectric layer onto silicon photonics platform solves this predicament. Piezoelectricity has been employed for tuning the cavity resonances of photonic crystal microcavities formed on silicon deformable membranes.[6] It has also been used in optical microelectromechanical systems (MEMS) actuation.[7] It has also been used for phase modulation in Mach–Zehnder interferometers based on silica (glass) waveguides to demonstrate optical switching.[8] In this work, piezoelectricity is applied to induce birefringence in standard SOI waveguides in order to fine tune the phase mismatch of nonlinear optical processes.

Among the various piezoelectric materials, lead zirconate titanate (PZT) was chosen because of its strong piezoelectric effect. PZT is widely used in creating ultrasonic transducers as well as MEMS devices and ferroelectric random-access memories.[7,9]

The device structure consists of an oxide-clad silicon waveguide and a PZT capacitor formed on top of it. The PZT capacitor consists of a thin film PZT layer sandwiched between a top and a bottom platinum electrode. The oxide cladding is required to minimize the optical absorption loss resulting from the bottom electrode. The anisotropic stress, or equivalently strain, induced by piezoelectric effect in PZT breaks the centrosymmetry of the silicon crystal and leads to material birefringence in silicon as governed by photoelastic effect. Modal birefringence Δn is defined as the difference between the effective indices of transverse electric (TE) and transverse magnetic (TM) waveguide modes. Three components contribute to Δn. The first component is due to the asymmetric geometry of the rib waveguide. The second term is associated with the material birefringence induced by the residual stress of the cladding layers (oxide, electrodes, and unbiased PZT) that cover the rib. The birefringence caused by these two components is not tunable and can be expressed as a constant Δn_0. The third component contributing to Δn is the tunable material birefringence Δn_{piezo} due to the tunable stress induced by an applied electric filed to the PZT layer. Consequently, $\Delta n = n_{\text{TE}} - n_{\text{TM}} = \Delta n_0 + \Delta n_{\text{piezo}}$. In turn, $\Delta n_{\text{piezo}} = (C_2 - C_1)(\sigma_{\text{piezo},X} - \sigma_{\text{piezo},Y})$, where C_1 and C_2 are the stress-optic coefficients related to the Young's modulus, Poisson's ratio, and the photoelastic tensor elements of the material.[3] $\sigma_{\text{piezo},X}$ and $\sigma_{\text{piezo},Y}$ are the x and y components of stress in the waveguide induced by the piezoelectric effect, respectively.

The stress distribution in the waveguide was simulated

[a)]Electronic mail: jalali@ucla.edu

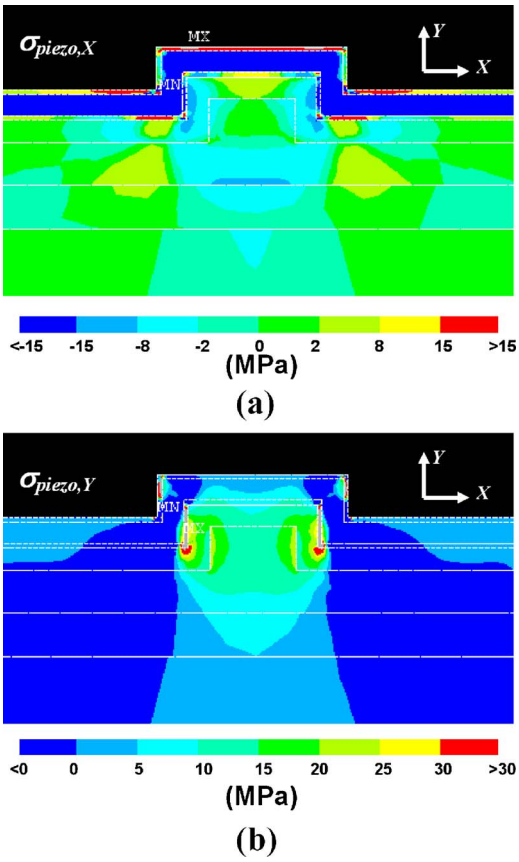

FIG. 1. (Color online) Stress distribution in (a) horizontal direction ($\sigma_{\text{piezo},X}$) and (b) vertical direction ($\sigma_{\text{piezo},Y}$) in the waveguide structure, when a voltage of 12 V is applied across the PZT capacitor.

by using a finite-element analysis package (ANSYS) which is capable of incorporating structural, material, electromagnetic, and piezoelectric analyses. An oxide-clad (500 nm thick) single-mode waveguide with width of 2 μm, rib height of 2 μm, and slab height of 1.1 μm was designed. The PZT thickness is chosen to be 500 nm, which gives rise a large difference between $\sigma_{\text{piezo},X}$ and $\sigma_{\text{piezo},Y}$, as determined from the ANSYS simulations. The platinum electrodes are 100 nm thick. Figures 1(a) and 1(b) show the stress distributions $\sigma_{\text{piezo},X}$ and $\sigma_{\text{piezo},Y}$, respectively, within the structure when a voltage of 12 V is applied across the PZT capacitor. It should be emphasized that the shown stresses are only the tunable component arising from the applied field to the PZT layer. In reality, there exists an additional stress induced by the strained cladding layers, which could have higher values.[3,4] However, this residual stress has a constant value, thus, it is not of interest in this work. The average values of $\sigma_{\text{piezo},X}$ and $\sigma_{\text{piezo},Y}$ within the waveguide core area are calculated to be -1 and $+12$ MPa, respectively. Hence, the stress-induced birefringence due to piezoelectric effect is estimated to be $\Delta n_{\text{piezo}} \approx 3 \times 10^{-4}$. As discussed later, this value is large enough to be useful in applications requiring dynamic tuning of birefringence.

We have developed a process for fabricating SOI waveguides integrated with PZT capacitors. The silicon waveguide (with same dimensions of the simulation) is patterned by standard photolithography and plasma dry-etch process. An oxide cladding layer (500 nm thick) is then deposited by plasma-enhanced chemical vapor deposition. On top of the oxide cladding, a 100 nm/10 nm Pt/Ti bilayer

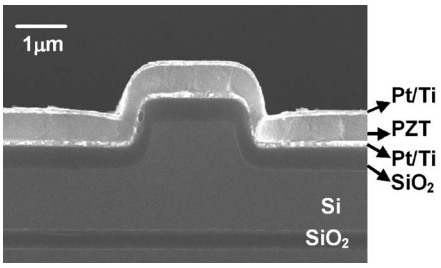

FIG. 2. SEM image of the fabrication waveguide structure with the PZT capacitor on top of it.

(the bottom electrode) is deposited by e-beam evaporation with a subsequent rapid thermal annealing (RTA) at 700 °C for 30 s in oxygen ambient.

We adopted radio-frequency magnetron sputtering technique to deposit a thin PZT film.[9] PZT sputtering is performed using a ceramic PZT (Zr/Ti=52/48) target at room temperature.[10] The 500 nm thick sputtered PZT film is then crystallized by RTA at 650 °C for 60 s in oxygen ambient to achieve the peroskite structure. The sputtered PZT film thickness deviates less than 50 nm along a 2 cm long waveguide as measured from scanning electron microscope (SEM) images. The right composition of the deposited PZT $[Pb(Zr_{0.52},Ti_{0.48})O_3]$ was confirmed with the Rutherford back scattering technique. X-ray diffraction pattern of the annealed PZT film was also studied. Typical peaks in the (111), (100), (110), and (200) directions are observed with a preferential orientation along the (111) direction. A 100 nm/10 nm Pt/Ti top electrode layer is finally deposited on top of the PZT layer by e-beam evaporation. Figure 2(b) shows a SEM image of the fabricated device structure at a cleaved facet.

We characterize the PZT film quality by measuring its piezoelectric and ferroelectric properties. The fabricated PZT thin film has a piezoelectric coefficient $d_{33}-130$ pC/N measured by normal load technique.[11] A ferroelectric hysteresis loop is also measured by Sawyer–Tower circuit[7] at 1 kHz. The remnant polarization is 20 μC/cm^2 and the coercive field is $\sim$55 kV/cm. These values are comparable with previously reported values of sputtered PZT thin films.[7,9]

We use the Fabry–Pérot (FP) resonance technique to measure the waveguide loss and more importantly the material birefringence induced in the waveguide by piezoelectricity. The input light from an external cavity tunable laser is coupled into and out of the 2 cm long waveguide by two identical objective lenses (numerical aperture=0.4). The polarization state is controlled by a polarizer positioned before the input of the waveguide. The silicon waveguide integrated with the PZT capacitor exhibits low linear propagation loss of 0.6 dB/cm.

The group indices $n_{g,\text{TE}}$ and $n_{g,\text{TM}}$ (for TE and TM modes, respectively) were measured from the free spectral range of FP resonances caused by reflection from the waveguide facets ($n_{g,\text{TE}} \approx n_{g,\text{TM}} = 3.63 \pm 0.01$). Taking the waveguide dispersion into account ($dn/d\lambda \sim 0.1\ \mu\text{m}^{-1}$ from BEAMPROP simulations), the effective refractive indices for TE and TM modes were extracted to be $n_{0,\text{TE}} \approx n_{0,\text{TM}} = 3.46 \pm 0.01$. We note that these values are consistent with the simulation results.

The wavelength shift for TE ($\Delta\lambda_{\text{TE}}$) and TM ($\Delta\lambda_{\text{TM}}$) modes in the FP spectra were measured when a dc bias was

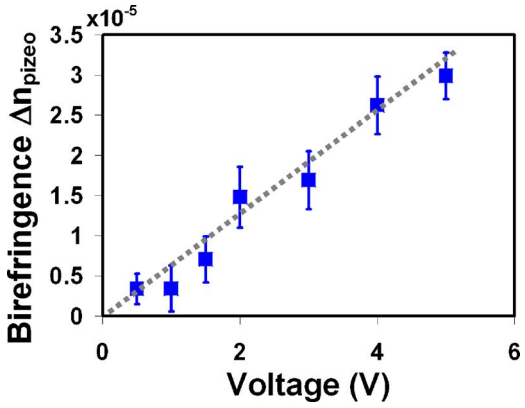

FIG. 3. (Color online) Birefringence of the waveguide due to piezoelectric effect from PZT as a function of dc voltages.

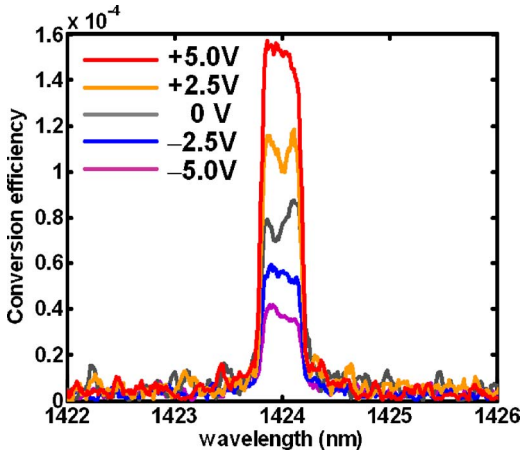

FIG. 4. (Color online) Anti-Stoke spectra of wavelength conversion based upon CARS at different dc bias applied to the PZT capacitor.

applied to the PZT capacitor. By using the relations $\Delta\lambda_{TE}/\lambda_{TE}=\Delta n_{TE}/n_{0,TE}$ and $\Delta\lambda_{TM}/\lambda_{TM}=\Delta n_{TM}/n_{0,TM}$, we can extract the stress-induced birefringence due to piezoelectric effect, i.e., $\Delta n_{piezo}=\Delta n_{TE}-\Delta n_{TM}$. Figure 3 presents this measured birefringence as a function of the dc voltage, showing a linear behavior. At the maximum bias of 5 V, the birefringence is measured to be $\Delta n_{piezo}=3\times10^{-5}\pm10^{-6}$. This is lower than the simulated value of 1.6×10^{-4} from ANSYS simulations. The discrepancy can be attributed to the fact that the PZT piezoelectric coefficients used in the simulation are taken from the bulk values, which are different from thin film values.[7] Also, the nonconformality of PZT and Pt/Ti films over the rib waveguide may have caused further complications. As discussed before, higher birefringence of 3×10^{-4} is predicted at a bias of 12 V. Unfortunately, the leakage current of the PZT capacitor in the present devices prevents applying voltages of above 5 V. Further optimization of the structural design resulting in larger difference between $\sigma_{piezo,X}$ and $\sigma_{piezo,Y}$ can enhance the birefringence tuning range.

The technology presented here will be applicable to recent and exciting developments in nonlinear silicon photonics. In particular, both coherent anti-Stokes Raman scattering (CARS) and Kerr-based wavelength conversion require phase matching.[2,12] The requisite zero dispersion can be achieved by engineering the waveguide dimensions such that the material dispersion is compensated by the contribution from the waveguide geometry,[13] or, as mentioned before, using birefringence. Nonetheless, it has been shown that the phase mismatch is a very sensitive function of errors in waveguide dimensions inevitably caused during device fabrication.[1] Dynamic tunability of birefringence in the order of 10^{-4} is sufficient for compensating an error of ~50 nm in waveguide dimensions.[1]

Figure 4 demonstrates this concept in the context of CARS wavelength conversion from the Stoke signal at 1.672 μm to anti-Stoke signal at 1.424 μm (TM polarized) using a pump source at 1.538 μm (TE polarized) with an input power of ~1.2 W. The increase in converted anti-Stoke power through fine tuning of birefringence by piezoelectricity is clearly demonstrated. We achieve ~5.7 dB efficiency tuning by varying the dc bias applied to the PZT capacitor from −5 to +5 V. The design of the present waveguides is far from phase matching. The total efficiency can be significantly improved by proper waveguide design such that it meets the phase matching condition.[1] Then, the present tuning technique can be used to correct the fabrication-induced phase mismatch and achieve high CARS conversion efficiency.

In summary, we have reported preliminary results on dynamic tuning of a silicon waveguide's birefringence using integrated PZT transducers. This capability with many promising applications require phase matching for efficient parametric processes. In particular, we demonstrate conversion efficiency improvement in CARS wavelength conversion using this technique. Dynamic tunability of waveguide dispersion relaxes the fabrication tolerances and also offers adaptive control of a waveguide's nonlinear response. Second-order nonlinearities are normally absent in silicon. By breaking the symmetry of the crystal, an integrated piezoelectric transducer may also offer a path to induce and control second-order optical nonlinearities in silicon.

This work is sponsored by DARPA under the EPIC program.

[1] D. Dimitropoulos, V. Raghunathan, R. Claps, and B. Jalali, Opt. Express **12**, 149 (2004).
[2] V. Raghunathan, R. Claps, D. Dimitropoulos, and B. Jalali, J. Lightwave Technol. **23**, 2094 (2005).
[3] D.-X. Xu, P. Cheben, D. Dalacu, A. Delâge, S. Janz, B. Lamontagne, M.-J. Picard, and W. N. Ye, Opt. Lett. **29**, 2384 (2004).
[4] R. S. Jacobsen, K. N. Andersen, P. I. Borel, J. Fage-Pedersen, L. H. Frandsen, O. Hansen, M. Kristensen, A. V. Lavrinenko, G. Moulin, H. Ou, C. Peucheret, B. Zsigri, and A. Bjarklev, Nature (London) **441**, 199 (2006).
[5] V. Raghunathan and B. Jalali, Proceedings of the Conference of Lasers and Electro-Optics (CLEO), Long Beach California, USA, 2006 (unpublished), Paper No. CMK5.
[6] C. W. Wong, P. T. Rakich, S. G. Johnson, M. Qi, H. I. Smith, E. P. Ippen, and L. C. Kimerling, Appl. Phys. Lett. **84**, 1242 (2004).
[7] N. Setter, *Electroceramic-based MEMS: Fabrication-Technology and Applications* (Springer, New York, 2005).
[8] S. Donati, L. Barbieri, and G. Martini, IEEE Photonics Technol. Lett. **10**, 1428 (1998).
[9] H. Ishiwara, M. Okuyama, and Y. Arimoto, *Ferroelectric Random Access Memories: Fundamentals and Applications* (Springer, New York, 2004).
[10] B. Jaffe, W. R. Cook, and H. Jaffe, *Piezoelectric Ceramics* (Academic, London, 1971).
[11] K. Lefki and G. J. M. Dormans, J. Appl. Phys. **76**, 1764 (1994).
[12] K. K. Tsia, S. Fathpour, and B. Jalali, Opt. Express **14**, 12327 (2006).
[13] M. A. Foster, A. C. Turner, J. E. Sharping, B. S. Schmidt, M. Lipson, and A. L. Gaeta, Nature (London) **441**, 960 (2006).